Enriched Expression of Serotonin 1B and 2A Receptor Genes in Macaque Visual Cortex and their Bidirectional Modulatory Effects on Neuronal Responses

Akiya Watakabe[1,2], Yusuke Komatsu[1], Osamu Sadakane[3], Satoshi Shimegi[3], Toru Takahata[1], Noriyuki Higo[4], Shiro Tochitani[1,2,7], Tsutomu Hashikawa[5], Tomoyuki Naito[3], Hironobu Osaki[3], Hiroshi Sakamoto[3], Masahiro Okamoto[3], Ayako Ishikawa[3], Shin-ichiro Hara[3], Takafumi Akasaki[3], Hiromichi Sato[3] and Tetsuo Yamamori[1,2,6]

[1]Division of Brain Biology, National Institute for Basic Biology, 38 Nishigonaka Myodaiji, Okazaki 444-8585, Japan, [2]Department of Basic Biology, Graduate University for Advanced Studies, 38 Nishigonaka Myodaiji, Okazaki 444-8585, Japan, [3]Laboratory of Cognitive and Behavioral Neuroscience, Graduate School of Medicine, Osaka University, Toyonaka 560-0043, Japan, [4]System Neuroscience Group, Neuroscience Research Institute, National Institute of Advanced Industrial Science and Technology, Umezono 1-1-1, Tsukuba 305-8568, Japan, [5]Laboratory for Neural Architecture, Brain Science Institute, RIKEN, Wako 351-0198, Japan and [6]National Institute for Physiological Sciences, 38 Nishigonaka Myodaiji, Okazaki 444-8585, Japan

[7]Current address: Anatomy and Developmental Neurobiology, Institute of Health Biosciences, University of Tokushima Graduate School, 3-18-15 Kuramotochou, Tokushima 770-8503, Japan.

Akiya Watakabe, Yusuke Komatsu, and Osamu Sadakane contributed equally to this work.

To study the molecular mechanism how cortical areas are specialized in adult primates, we searched for area-specific genes in macaque monkeys and found striking enrichment of serotonin (5-hydroxytryptamine, 5-HT) 1B receptor mRNA, and to a lesser extent, of 5-HT2A receptor mRNA, in the primary visual area (V1). In situ hybridization analyses revealed that both mRNA species were highly concentrated in the geniculorecipient layers IVA and IVC, where they were coexpressed in the same neurons. Monocular inactivation by tetrodotoxin injection resulted in a strong and rapid (<3 h) downregulation of these mRNAs, suggesting the retinal activity dependency of their expression. Consistent with the high expression level in V1, clear modulatory effects of 5-HT1B and 5-HT2A receptor agonists on the responses of V1 neurons were observed in in vivo electrophysiological experiments. The modulatory effect of the 5-HT1B agonist was dependent on the firing rate of the recorded neurons: The effect tended to be facilitative for neurons with a high firing rate, and suppressive for those with a low firing rate. The 5-HT2A agonist showed opposite effects. These results suggest that this serotonergic system controls the visual response in V1 for optimization of information processing toward the incoming visual inputs.

Keywords: 5-HT, activity-dependent, area-specific, monocular deprivation, primate, visual cortex

Introduction

Primates have highly complex cerebral cortices compared with other mammals. One characteristic feature of the primate cortex is the highly developed visual system. For example, at least 32 visual areas have been distinguished in the neocortex of primates (Felleman and Van Essen 1991). Among the visual areas, V1 (primary visual area) is considered to be one of the earliest functional subdivisions that existed in the cortex of the ancestral mammals (Northcutt and Kaas 1995). During the course of evolution, however, there appear to have emerged considerable differences in the functional architecture and intracortical connectivity of V1 across species (see e.g., Zarrinpar and Callaway 2006; Van Hooser 2007). The monkey V1 also has come to exhibit a highly laminated structure (Lund 1988), which reflects the structural separation of the different types of visual information (e.g., Sincich and Horton 2005). In our previous study, we identified *occ1/frp* mRNA as a molecule that is highly enriched in the macaque V1 (Tochitani et al. 2001; Yamamori and Rockland 2006). Interestingly, the area-specific expression patterns of the *occ1* mRNA were observed in macaques and marmosets but not in the other species examined (Takahata et al. 2006). On the basis of the existence of such a gene, we hypothesized that there may be a set of genes that contribute to the structural and functional specializations of the primate visual system. If such genes do exist, the identification and characterization of their functions in V1 will markedly contribute to our understanding of the mechanisms of primate vision.

To examine this possibility, we first carried out a new round of screening in search of genes with V1-enriched expression among macaque neocortical areas and found that the 5-HT (5-hydroxytryptamine, serotonin) 1B receptor mRNA is highly enriched in V1. In addition, we also found that the 5-HT2A receptor mRNA exhibits an area/lamina pattern very similar to that of the 5-HT1B receptor mRNA at the V1/V2 border, which is consistent with previous reports (Burnet et al. 1995; Lopéz-Giménez et al. 2001). 5-HT1B and 5-HT2A receptors belong to G-protein–coupled receptors and activate a cascade of intracellular signaling events (reviewed in Baumgarten and Gothert 1997; Barnes and Sharp 1999; Sari 2004). They are involved in neuropsychiatric disorders, as well as in a wide

variety of physiological functions in different systems. The 5-HT1B receptor, in particular, has been reported to modulate neurotransmission in various pathways, such as the retinocollicular (Mooney et al. 1994), retino-suprachiasmic nuclear (Pickard et al. 1999), and thalamocortical (Laurent et al. 2002) pathways. The monkey V1 is densely innervated by serotonergic terminals (de Lima et al. 1988) and possesses abundant 5-HT radioligand binding sites (Rakic et al. 1988; Parkinson et al. 1989). Considering the enhanced expressions of 5-HT1B and 5-HT2A receptor genes in V1, it is likely that the two 5-HT receptors play important roles in modulating neurotransmission in V1.

The macaque V1 has been an excellent model system for studying the functional organization of the primate cortex, in which stimulus-evoked responses can be manipulated by controlling external stimuli. A wealth of information on the basic electrophysiological properties (Hubel and Wiesel 1977) and anatomical circuitry of V1 neurons is available (Lund 1988; Callaway 1998) and accumulating to date. Supported by these previous studies, we wanted to understand the functional meaning of V1-specific expression of the two 5-HT receptor genes. First, we wanted to determine what anatomical structures are associated with the expressions of the 5-HT1B and 5-HT2A receptor mRNAs. Results of the in situ hybridization (ISH) study showed that these mRNAs are highly enriched in the excitatory neurons in geniculorecipient layers IVA and IVC. Interestingly, we found that activity-driven regulation plays a key role in this lamina specificity, as is found for cytochrome oxidase (CO) (Wong-Riley 1994) or *occ1* mRNA (Tochitani et al. 2001) expressions. Second, we wanted to determine the functional significance of this enriched expression using electrophysiological and pharmacological techniques (Sato et al. 1996; Ozeki et al. 2004). Here, we provide evidence that 5-HT1B and 5-HT2A receptor agonists modulate neuronal responses in V1. Altogether, our results suggest the importance of the serotonergic system in modulating the behavior of V1 neurons, and that the V1-enriched expression of the two 5-HT receptor genes should provide a basis for the functional specialization of the primate V1.

Materials and methods

Anatomy

Experimental Animals

For restriction landmark cDNA scanning (RLCS) and semiquantitative reverse transcription–PCR (RT-PCR) analysis, postmortem brain tissues of African green monkeys (*Cercopithecus aethiops*) were obtained from the Japan Poliomyelitis Research Institute, as previously described (Tochitani 2001; Watakabe et al. 2001; Komatsu et al. 2005). For ISH experiments, the brains of 8 adult macaques, 7 Japanese monkeys (*Macaca fuscata*) and 1 crab-eating monkey (*Macaca fascicularis*), were used. These monkeys were perfused through the hearts with 4% paraformaldehyde under anesthesia, and thus considered to be a minimum postmortem period before tissue fixation. Monocular inactivation for 21 days was performed as previously described (Tochitani et al. 2001). Four nontreated monkeys were used for ISH experiments and 4 monkeys were used for tetrodotoxin injection; 1 monkey for each experiment of 21 days, 1 day, 6 and 3 h monocular inactivation. Part of sections from the same monkey brains (2 nontreated monkeys and one with tetrodotoxin injection for 21 days) used in previous studies (Tochitani et al. 2001; Takahata et al. 2006) was used. All the experiments described here were performed in compliance with the guidelines for animal experiments of the National Institutes of Natural Sciences, Japan and the National Institutes of Health, USA.

RLCS and Semiquantitative RT-PCR Analyses

RLCS was carried out essentially the same as described previously (Suzuki et al. 1996; Shintani et al. 2004) using poly (A)+ RNA purified from 4 (frontal, motor, temporal, and visual) areas depicted in Figure 1*A*. In this analysis, mRNAs from these areas were converted to double-stranded cDNA by reverse transcription and digested with *Bcl*I (first dimension) and *Hin*fI (second dimension) for 2-dimensional gel electrophoresis (Fig. 1*B*). The 4 cDNA samples were electrophoresed simultaneously in a single run and the patterns of spots were compared visually by 3 independent persons. Five candidates were chosen for gene identification and RT-PCR analyses. One spot, which we identified as the 3′-untranslated region (UTR) of 5-HT1B receptor gene (see below for detail), showed the largest area differences among the 5 spots and used for subsequent analyses. Detailed description of the method and the genes obtained by this screening will be published elsewhere (Y. K. and T. Y., unpublished data).

Identification of 5-HT1B Receptor in RLCS Spots

The cDNA spot cloned from the RLCS analyses was used to screen a cDNA library constructed using the poly (A)+ RNA purified from the monkey visual cortex. All the positive clones obtained by this screening matched the human genome sequence downstream of the 5-HT1B receptor gene locus. The longest clone, RC15i, contained the sequence spanning position 2764–4260 (coding sequence [CDS] = pos. 1–1173). Because 5-HT1B receptor mRNA is longer than 28S ribosomal RNA (4.7 kb) (Jin et al. 1992), it was likely that the RLCS spot corresponds to the 5-HT1B receptor. Therefore, we conducted semiquantitative RT-PCR using the primer sets within the cDNA retrieved from the RLCS gel (data not shown) and within the coding sequence for the 5-HT1B receptor (Fig. 1*A*). RT-PCR with both primers showed the same visual area–specific pattern. Furthermore, ISH was carried out using 3 nonoverlapping probes: RC15i, containing the putative 3′-UTR region (pos. 2764–4260), the coding sequence of the 5-HT1B receptor gene (pos. 150–571), and a different region of the coding sequence with 3′-UTR (pos. 616–1599). All 3 probes showed the same ISH patterns (data not shown). From these results, we concluded that this spot identified by the RLCS analysis is the product of the 5-HT1B receptor gene.

Monocular Inactivation

Monocular inactivation for shorter time periods (3–24 h) was performed with slight modification in anesthesia as follows. Briefly, monkeys were anesthetized with ketamine (6 mg/kg) and medetomidine (0.25 mg/kg) by intramuscular injection (i.m.). Tetrodotoxin (15 μg dissolved in 10 μL of saline) was injected manually into the vitreous cavity of the left eye using a Hamilton syringe over 5 min and the syringe was left in position for further 15 min. After injection, the loss of the pupillary reflex in the injected eye was confirmed. The effect of medetomidine was then reversed by intramuscular injection of atipamezole (1.25 mg/kg). The reversal effect was very quick and the monkey was almost fully recovered after 10 min of atipamezole injection, suggesting that the effect of ketamine had been already gone at that time point. After 2.5 h of atipamezole injection (approximately 3 h after tetrodotoxin injection), the monkey was administered with ketamine (6 mg/kg, i.m.) followed by an overdose of Nembutal (at least 100 mg/kg body weight) and perfused intracardially with 4% paraformaldehyde in 0.1 M phosphate buffer (pH 7.4).

In Situ Hybridization

The probes used in the ISH experiments were cloned by RT-PCR using RNA from a rhesus monkey (Supporting Table S1). For the 5-HT1B receptor, we prepared the 3 different probes described above and used either mixed or separately. We also conducted ISH for the sense probes of each gene to confirm the specificity of hybridization (data not shown).

The tissue sections were made on freezing microtome (15-μm thickness for double ISH, and 35- to 40-μm thickness for single ISH and histochemical staining). CO staining was performed as previously
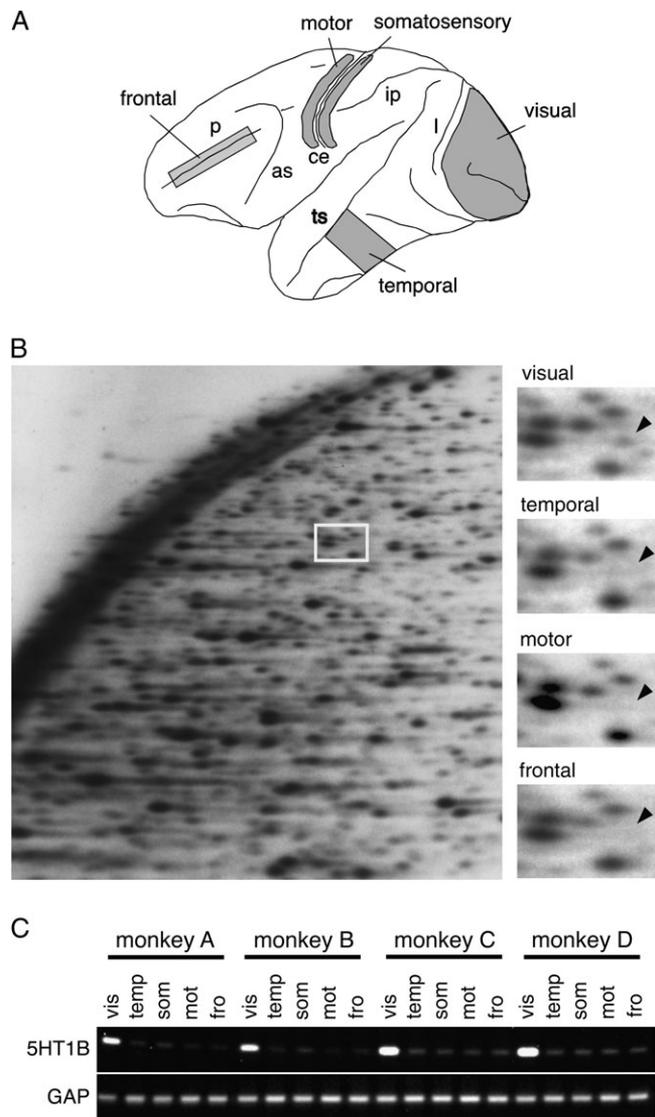
Figure 1. Identification and confirmation of 5-HT1B receptor as V1-specific gene. (*A*) Monkey neocortical areas used in this study are shown. The left hemisphere of the cerebral cortex is shown. Anterior is to the left and posterior to the right. Major sulci are shown by lowercase letters: p, principal sulcus; as, arcuate sulcus; ce, central sulcus; ip, intraparietal sulcus; ts, superior temporal sulcus; and l, lunate sulcus. (*B*) RLCS analysis of the monkey neocortex. Four distinct regions of the monkey neocortex depicted in panel A were analyzed. The left panel shows an example of a 2-dimensional gel of RLCS analysis. The area corresponding to the white box contained a spot present only in the visual area (shown by arrowhead) but not in temporal, motor and frontal areas. (*C*) Semiquantitave RT-PCR demonstrated that the 5-HT1B receptor mRNA expression level was high in the visual (vis) cortex, and very low in the temporal (temp), somatosensory (som), motor (mot) or frontal (fro) areas. The same specificity for the visual cortex was observed in 4 different individual monkeys. The glyceraldehyde-3-phosphate dehydrogenase gene ubiquitously expressed across areas was used as control.

described (Wong-Riley 1994). ISH was carried out as described previously with minor modifications (Tochitani et al. 2001). Free-floating sections were treated with 10 µg/mL proteinase K for 30 min at 37 °C. After acetylation, the sections were incubated in a hybridization buffer containing 0.5–1.0 µg/mL digoxigenin (DIG)-labeled probes at 60 °C. Hybridized sections were first washed in 2× SSC/50% formamide/0.1% *N*-lauroylsarcosine at 50 °C and treated with RNase A. After RNase treatment, the sections were further washed in 2× SSC/0.1% *N*-lauroylsarcosine and in 0.2× SSC/0.1% *N*-lauroylsarcosine at 37 °C. Hybridization signals were visualized by alkaline phosphatase immunohistochemistry followed by

nitro blue tetrazolium/5-Bromo-4-chloro-3-indolyl phosphate (NBT/BCIP) detection (Roche Diagnostics, Tokyo, Japan).

For the double ISH, DIG-, and fluorescein isothiocyanate (FITC)–labeled antisense probes were prepared and used for ISH. Hybridization was carried out as described above in the presence of both DIG- and FITC-labeled riboprobes. The fluorescence detection of the hybridization signals was performed as described previously (Komatsu et al. 2005; Watakabe et al. 2007). Cell counting in Figure 4 and supporting Table S2 was performed as described previously (Watakabe et al. 2007) in a column of 172 µm (400 pixel) taken from double-stained tissue sections (15 µm thickness) of V1 from 3 different monkeys. Layers were determined on the basis of morphology and density of VGluT1-mRNA-positive neurons.

Electrophysiology

Experimental Animals

Two adult macaques, *M. fuscata*, were used. Details of the experimental preparation are previously described (Sato et al. 1996; Ozeki et al. 2004). The animals were anesthetized with ketamine (10 mg/kg, i.m.) followed by a mixture of isoflurane (2.5–3.5%) and N_2O-O_2 (2:1). The trachea of each animal was intubated and a catheter was placed in the femoral vein. The animals were then placed in a stereotaxic head holder, continuously paralyzed with pancuronium bromide (0.1 mg/kg/h, i.v.) to minimize eye movements, and maintained under artificial ventilation. During the recording of neuronal activity, isoflurane dose was reduced to 0.3–0.7% in N_2O:O_2 (2:1), and fentanyl citrate (Fentanest, Sankyo, Tokyo, Japan; 10 µg/kg/h, i.v.) and droperidol (Droleptan, Sankyo, Tokyo, Japan; 125 µg/kg/h, i.v.) were continuously infused. This treatment induced a state of neuroleptoanalgesia in the animals. It enabled us to record visual responses of nearly normal cortical activity and minimized the effect on mRNA expression which is regulated in an activity-dependent manner. Only when the heart rate of the animals exceeded more than 200 beats per min, sodium pentobarbital (2–5 mg/kg/h, i.v.) was also added to the infusion solution. A local anesthetic, lidocaine, was administered at pressure points and around surgical incisions. Rectal temperature and the end-tidal CO_2 level were adjusted to 37–38 °C and 3.5–4%, respectively. All electrophysiological procedures were carried out in accordance with the guidelines for animal experiments of the Osaka University School of Medicine, Japan and the National Institute of Health, USA.

Microiontophoresis

Drugs were administered iontophoretically via multibarreled glass electrodes attached to a recording pipette. Triple- or 4-barreled glass micropipettes were used for extracellular single-neuron recording and the iontophoretic administration of the 5-HT1B receptor-specific agonist CP93129 dihydrochloride (Tocris, Bristol, UK; 100 mM, pH 3.6), the 5-HT1B receptor-specific antagonist SB216641 hydrochloride (Tocris; 20 mM, pH 4.0), 5-HT2A receptor-agonist DOI (Sigma-Aldrich, St Louis, MO; 100 mM, pH 5.5), 5-HT2A receptor-specific antagonist ketanserin (Tocris, Ellisville, MO; 10 mM, pH 5.5), and the Ringer's solution to the neurons under study (Sato et al. 1996). The tip of the recording electrode protruded by 10–30 µm from the tip of the drug pipettes. The strength of the ejection currents of drugs and the Ringer's solution was between +1 and +60 nA. The retaining current was between −5 and −15 nA. No cells showed changes in spike size and firing frequency during the iontophoretic administration of the Ringer's solution. We recorded neuronal responses to stimulation with sinusoidal-grating patch with optimal stimulus parameters (Akasaki et al. 2002). Peristimulus time histograms (PSTHs) of spike responses were constructed during 6–10 times of stimulus presentations before (control condition), during (drug condition) and after (recovery condition) the drug administration. Only neurons whose response level was recovered to the control level after cessation of drug administration ($P > 0.05$, Mann–Whitney's U test) were included in our results. In further analysis, the responses in the control and recovery conditions were averaged and, then, the average was compared with the responses during drug administration by Mann–Whitney's U test. Statistically significant increment and decrement of responses were classified as response facilitation and suppression, respectively. The

recording pipette was filled with 0.5 M sodium acetate containing 4% Pontamine Sky Blue. At the end of each penetration, dye marks were produced by passing tip-negative DC current (intensity: 8–10 μA, duration: 1 s at 0.5 Hz, 100 pulses) and recovered in histological sections (see below). After recording, the animals were deeply anesthetized with sodium pentobarbital (50 mg/kg, i.v.) and perfused transcardially with buffered saline followed by 4% paraformaldehyde in saline. Thin cortical sections were sliced at 60-μm thickness in the parasagittal plane and stained with cresyl violet, and the locations of the recorded sites were identified by microscopic observations. In 1 case, the cortical sections obtained from 1 of the experimental monkeys were used to perform ISH of 5-HT1B and 5-HT2A genes, which showed that their mRNAs were not significantly downregulated during the recording periods.

Visual Stimulation

When a neuron was encountered to respond to visual stimuli, the positions and sizes of the receptive fields of the recorded cells were manually plotted using a hand-held projector on a tangent screen placed 57 cm in front of the eyes of the animal. Subsequently, the receptive field properties, such as dominant eye, optimal orientation and direction of stimulus, spatial frequency, ON/OFF characteristics with respect to a stationary flashed bar, and tuning to stimulus length and velocity were assessed with the hand-held projector. Then a computer-generated visual stimulus was presented on a CRT monitor (CPD-G500J, SONY; Tokyo, Japan; mean luminance 40 cd/m^2; screen size, 40 × 30 cm^2; resolution, 1024 × 768 pixels; and refresh rate, 100 Hz), which was placed 57 cm from the animal. The visual stimuli were generated by a visual stimulation system VSG 2/3 (Cambridge Research System, Rochester, UK) and controlled by an IBM-PC/AT compatible computer using custom-made software. The visual stimulus consisted of a drifting circular grating patch with optimal orientation, spatial frequency, and velocity, which covered a cell's receptive field. The effects of drugs were tested for either the visual responses or spontaneous firings. Each stimulus was drifted for 2 s and interleaved for 1 s with a blank screen of the same mean luminance (40 cd/m^2) as that of the gratings. Either complex or simple cell was classified according to the ratio of the first harmonic (F1) to the mean (F0) of the response to a drifting grating stimulus (F1/F0 > 1, simple cell; F1/F0 < 1, complex cell) (Skottun et al. 1991).

Results

Identification of 5-HT1B Receptor as V1-Specific Gene

To screen area-specific molecules systematically in the monkey neocortex, we carried out a new round of screening by the RLCS method (Suzuki et al. 1996; Shintani et al. 2004). In this analysis, mRNAs were purified from 4 distinct cortical areas (Fig. 1A), converted to cDNA by reverse transcription and digested with a pair of restriction enzymes for 2-dimensional analysis (Fig. 1B). Among the spots that showed area difference, we cloned a gene that is specifically expressed in the visual area (Fig. 1B), which turned out to be the 5-HT1B receptor gene (see Materials and Methods). Semiquantitative RT-PCR analysis using primers for the coding sequence of the 5-HT1B receptor gene confirmed its specific expression in the visual area (Fig. 1C).

To examine the distribution of 5-HT1B receptor mRNA in the monkey brain in more detail, we carried out ISH analyses. The expression was strikingly high in V1 and the lateral geniculate nucleus (LGN) (Fig. 2C,E). Because the mRNA expression was low in the extrastriate cortex, the abrupt change in the intensity of mRNA staining was observed at the border between V1 and V2 (Fig. 2F). Within V1, the expression of 5-HT1B receptor mRNA was mostly confined to layers IVA and IVC, the major geniculocortical input layers, and was particularly strong in the lower part of layer IVCbeta (Fig. 2H).

In addition, the expression was also observed at lower intensity in layers II/III and VI of V1, which also receive geniculocortical inputs to a lesser extent. In the LGN, the strong mRNA expression was observed in all 6 layers, and there was no significant difference in staining intensity between the magnocellular and parvocellular layers (Supporting Figs S1 and S3).

Compared with the strong expression in V1, the expression of 5-HT1B receptor mRNA in other primary sensory areas was much weaker. Nonetheless, the ISH signals were localized in the middle layers (likely to be layer IV) as in V1 and significantly higher than the surrounding areas (Fig. 2C, A1 and S1 for auditory and somatosensory cortices, respectively; see also Fig. 3 and supporting Fig. S1O). There were also expressions at lower levels throughout the neocortex. The expression was generally restricted to the upper layers. In addition, in the motor and insular cortices, layer 5 pyramidal neurons also expressed 5-HT1B receptor mRNA at a low level (Fig. 3, M1 and IPro). In the entorhinal cortex, 5-HT1B receptor mRNA was expressed in layers V and VI (Fig. 3, Ent).

In addition, we observed the 5-HT1B receptor mRNA expression in various subcortical structures, such as the non-visual thalamus, parabigeminal nucleus, and ventral striatum (Fig. 2C,D, Th, Pul, and PBG; see supporting material for detailed account of the 5-HT1B receptor mRNA distribution).

Overall, however, the 5-HT1B receptor mRNA expression was by far the most conspicuous in V1, followed by that in the LGN. To date, 14 genes encoding different 5-HT receptors have been identified in the human genome (Hoyer et al. 2002). To test whether other 5-HT receptors exhibit an expression pattern similar to that of 5-HT1B receptor mRNA, we cloned the cDNA of each 5-HT receptor in macaques and carried out ISH. Table 1 shows the summary of the result for thirteen 5-HT receptor genes, for which we obtained the reliable ISH data. Among the 13 genes, we detected the expressions of 5-HT1A, 5-HT1E, 5-HT2A, 5-HT2C, 5-HT3A, and 5-HT6 receptor mRNAs in V1 in addition to 5-HT1B receptor mRNA. Among these genes, 5-HT2A receptor mRNA exhibited area and lamina preferences similar to those of 5-HT1B receptor mRNA (Table 1, Figs 4 and 5), although its expression was moderate all across areas.

Coexpression of 5-HT1B and 5-HT2A Receptor mRNAs in the Excitatory Neurons in Layer IVC of V1

The dense distribution of both 5-HT1B and 5-HT2A ISH signals in layer IVC of V1 raised a question as to whether these genes are coexpressed in the same neurons. To check this point directly, we performed fluorescence double ISH of 5-HT1B and 5-HT2A receptor genes (Fig. 4). This experiment revealed that these genes are strongly expressed in geniculorecipient layers IVA and IVC (Fig. 4B). 5-HT1B receptor mRNA was mostly confined to these layers, whereas 5-HT2A receptor mRNA was more widely distributed across layers. Therefore, many neurons expressed only the 5-HT2A receptor mRNA outside layers IVA and IVC, whereas both mRNAs were coexpressed within the same neurons in layers IVA and IVC.

We next asked which types of neurons expressed these 5-HT mRNAs, by performing the double ISH using VGluT1 for excitatory neurons (Bellocchio et al. 2000; Takamori et al. 2000; Komatsu et al. 2005) and GAD67 for inhibitory ones (Hendrickson et al. 1994). We found that the vast majority of the neurons that expressed 5-HT1B or 5-HT2A receptor mRNAs were the VGluT1 mRNA-positive excitatory neurons (Fig. 5, supporting Table S2), whereas a small population of
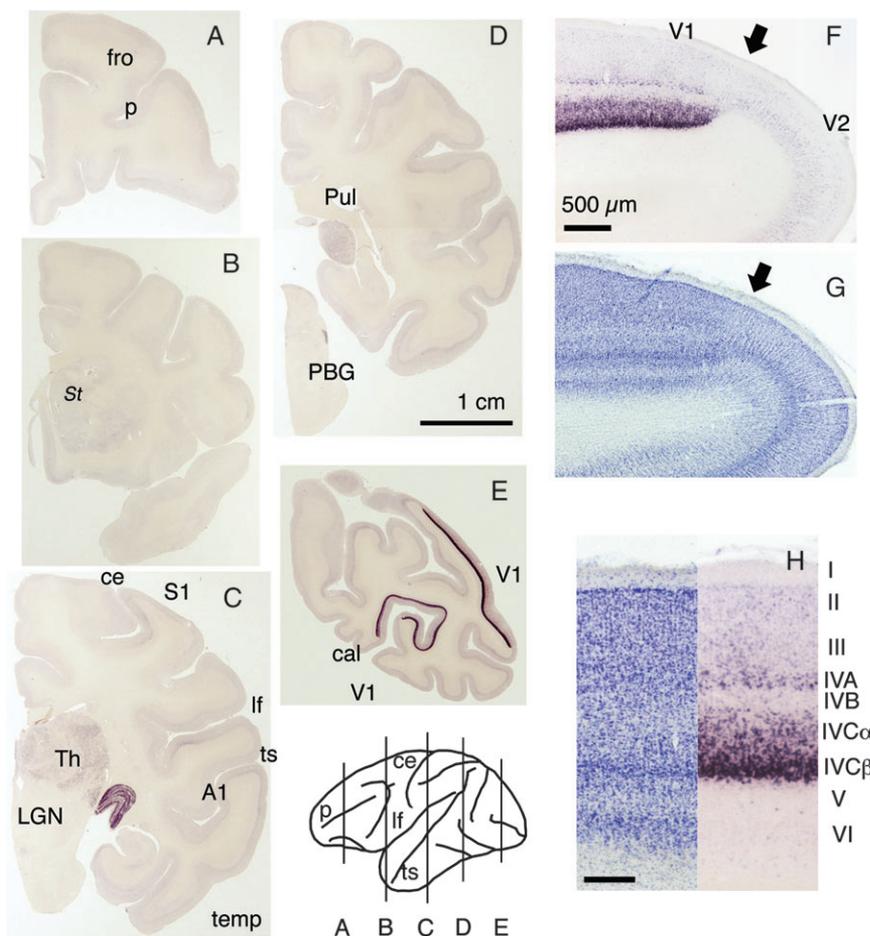
Figure 2. ISH analysis of 5-HT1B receptor mRNA. (*A*–*E*) Coronal sections of an adult monkey brain were prepared from the positions as depicted. Bar: 1 cm. Several areas are shown. Fro, frontal area; temp, temporal area; S1, primary somatosensory area; A1, primary auditory area. PBG, parabigeminal nucleus; Pul, pulvinar nucleus; St, striatum. Major sulci are shown by lowercase letters: p, principal sulcus; cal, calcarin sulcus; ce, central sulcus; lf, lateral fissure; ts, superior temporal sulcus. (*F*) 5-HT1B receptor mRNA expression at the V1/V2 border (shown by the black arrow). Bar: 500 μm. (*G*) The adjacent Nissl-stained section. (*H*) 5-HT1B receptor mRNA expression in V1. Bar: 200 μm.

5-HT mRNA-positive neurons were VGluT1-negative inhibitory neurons (Fig. 5, white arrows).

Next, we examined the percentages of VGluT1-positive neurons that coexpress 5-HT1B or 5-HT2A receptor mRNAs for each layer. The neurons with 5-HT1B receptor mRNA were mostly restricted to layers IVA, IVCalpha, and IVCbeta, where they constituted approximately 22.8 ± 3.5, 75.9 ± 3.5, and 70.4 ± 0.6% (mean ± SEM; $n = 3$) of the VGluT1-positive excitatory neurons, respectively (Fig. 5A). In layers II, III, V, and VI, 5-HT1B receptor mRNA was expressed in less than 5% of the excitatory neurons.

Compared with the 5-HT1B receptor mRNA, the 5-HT2A receptor mRNA was more widely expressed across layers. In layer IVC, the 5-HT2A receptor mRNA was expressed in approximately 80% of the excitatory neurons, which ratio is similar to the 5-HT1B mRNA. The percentage of the excitatory neurons expressing the 5-HT2A receptor mRNA decreased to 45–50% in layers III and V (Fig. 5B). The mRNA level per cell also appeared to be decreased in these layers. Thus, the layer IVC–enriched expression of the 5-HT2A receptor mRNA is considered to be due to the higher proportion of positive cells and the high level of mRNA expression within each cell. 5-HT2A receptor ISH signals were barely detectable in the excitatory neurons in layer VI.

5HT1B and 5HT2A receptor mRNAs were also detected in GAD67 mRNA-positive inhibitory neurons (Supporting Fig. S2). But the ratio of 5-HT1B and 5-HT2A–positive neurons among the GAD67-positive cells were quite low, being 5% and 11%, in our preliminary counting, respectively.

Activity-Dependent Regulation of 5-HT1B and 5-HT2A Receptors

The enriched expression of 5-HT1B and 5-HT2A receptor mRNAs in the geniculorecipient layers raises a possibility that their expressions are controlled by the activity transmitted through the retino-geniculate pathway, as is known for high enzymatic activity of CO, an indicator of neuronal activity (Wong-Riley 1994), and for *occ1* mRNA that shows similar layer specificity and activity dependency for the expression in V1 (Tochitani et al. 2001). To directly test this, we injected tetrodotoxin into 1 eye of a monkey to deprive retinal activity (Wong-Riley 1994) and examined whether the mRNA expressions of the two 5-HT receptors are affected. As Figure 6 shows, monocular inactivation caused a marked change in the expression of the two 5-HT receptor mRNAs. After 21 days of monocular inactivation, the expressions of both 5-HT1B (Fig. 6C) and 5-HT2A (Fig. 6D) receptor mRNAs were strongly downregulated in the column in layer IV that corresponded to
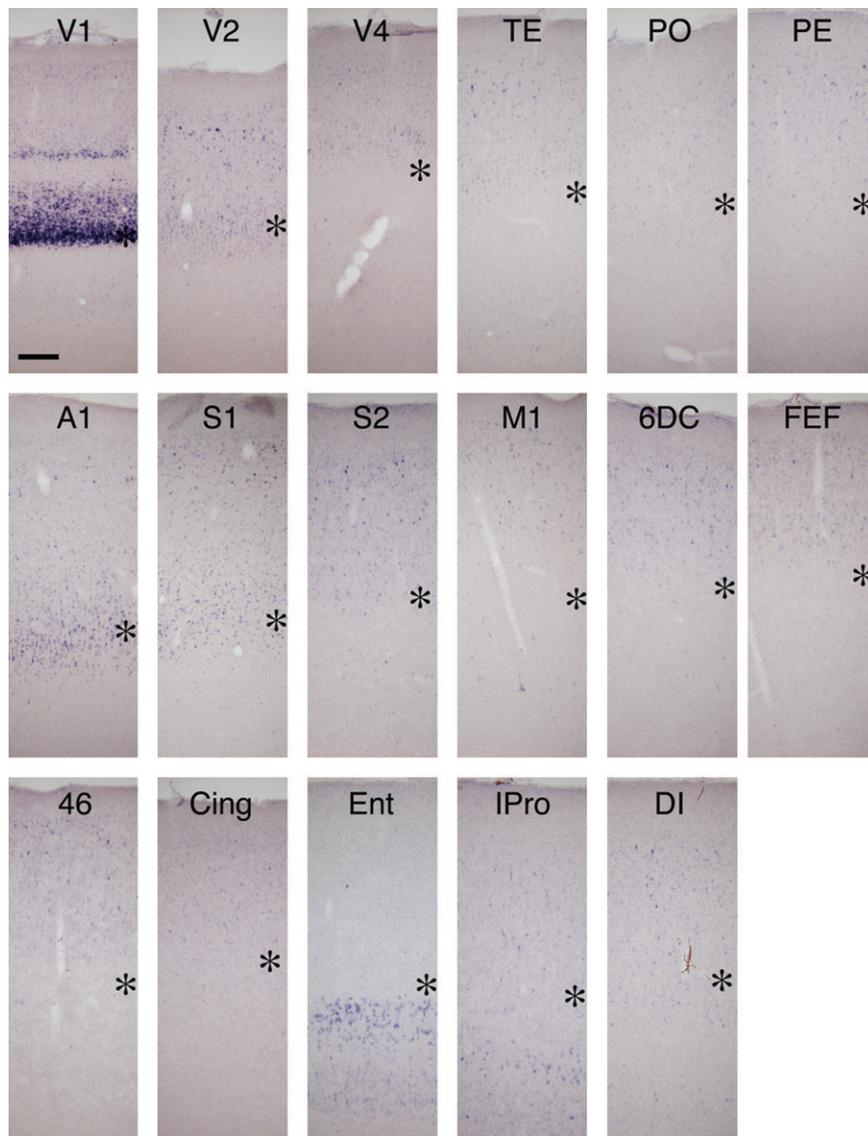
Figure 3. 5-HT1B receptor mRNA expression in various cortical areas. The expression of 5-HT1B receptor mRNA was examined in various cortical areas. The asterisks indicate the presumptive layer IV. V2; secondary visual area, V4; area V4 on the prelunate gyrus, TE; area TE in the inferior temporal gyrus, PO; area PO, PE; area PE (area 7) on the superior parietal lobule, A1; primary auditory area, S1; primary somatosensory area (area 3b) facing the central sulcus, S2; secondary somatosensory area, M1; primary motor area, 6DC; area 6DC or premotor area, FEF; frontal eye field (area 8), 46; area 46 on the bank of principle sulcus, Cing; cingular cortex (area 23), Ent; entorhinal cortex, IPro; insular proisocortex, DI; dysgranular insular cortex. Scale Bar: 200 μm.

the inactivated eye in a similar manner to that observed in CO staining (Wong-Riley 1994) (Fig. 6A) or in the *occ1* mRNA distribution (Fig. 6B). Activity-dependent expression of 5-HT1B receptor mRNA was also observed in the LGN (Supporting Fig. S3). To determine time required for the monocular inactivation to take effect, we examined shorter periods of monocular inactivation (1 day, 6 and 3 h). The downregulation of 5-HT1B and 5-HT2A receptor mRNAs in V1 occurred even after only 3 h of monocular inactivation (Fig. 6E,F). These results suggest that the V1-specific expression patterns of 5-HT1B and 5-HT2A receptor mRNAs are sustained by the ongoing visual activity.

Effects of 5-HT1B- and 5-HT2A Agonist/Antagonist on Visual Responses in V1

To directly examine the functional roles of 5-HT1B and 5-HT2A receptors in vivo, we conducted single-unit recordings of V1 neurons of anesthetized and paralyzed adult macaques, in conjunction with the microiontophoretic administration of specific agonists and antagonists of 5-HT1B and 5-HT2A receptors (5-HT1B agonist, CP93129; 5-HT1B antagonist, SB216641; 5-HT2 agonist, DOI; 5-HT2A antagonist, Ketanserin). The results of CP93129 (5-HT1B agonist) in 45 neurons and DOI (5-HT2A agonist) in 44 neurons are summarized in Figures 7 and 8, respectively.

Figure 7A shows the magnitude of visual responses of V1 neurons to a drifting sinusoidal-grating patch in which responses during iontophoresis of the 5-HT1B agonist, CP93129, were plotted against control responses. Of the 45 neurons recorded, 33 showed significant changes in firing rates during the CP93129 administration (P < 0.05, Mann–Whitney's U test), and in most of them (25 of 33), the effect of CP93129 was facilitative (Fig. 7A). Eight neurons showed suppressive

Table 1
Expression of various 5-HT receptor genes in V1, V2, and LGN

5-HT	1A	1B	1D	1E	1F	2A	2B	2C	3A	3B	4	6	7
<<V1>>													
Layer I	−	−	−	−	−	−	−	−	−	−	−	−	−
Layer II/III	B	+	−	+	−	++	−	S	−	−	−	+	+/−
Layer IVA	−	+++	−	−	−	+++	−	−	−	−	−	−	−
Layer IVB	−	−	−	−	−	+	−	−	−	−	−	−	−
Layer IVCalpha	−	++	−	−	−	+++	−	−	−	−	−	−	−
Layer IVCbeta	−	++++	+/−	−	+/−#	++++	−	−	−	−	−	−	−
Layer V	−	−	−	+	−	++	−	−	+	−	+/−	+/−	−
Layer VI	+	+/−S	−	+	−	+	−	+	+/−	−	−	+	−
<<V2>>													
Layer I	−	−	−	−	−	−	−	−	−	−	−	−	−
Layer II/III	++	+	−	+	−	++	−	S	−	−	−	+	+/−
Layer IV	−	+	−	−	+/−#	+++	−	−	−	−	−	−	−
Layer V	−	−	−	+	−	++	−	++	+	−	+	+/−	−
Layer VI	+	−	−	+	−	+	−	−	+/−	−	−	+	−
<<LGN>>													
Magno	+	++	+/−	+	−	−	−	−	−	−	−	+	I
Parvo	−	++	+/−	+	−	−	−	−	−	−	−	+	I

Note: ISH analyses for the known 5-HT receptor genes except for the 5-HT5B receptor gene, which is reported to be nonfunctional in humans, are shown. Although we also tested the 5-HT5A receptor gene, we observed a high background and did not obtain specific hybridization signals. For 5-HT2B and 5-HT3B receptor genes, no specific hybridization signals were observed in the sections tested. For the other receptors, we observed specific hybridization signals in certain brain regions. The intensities described here were rated from the relative intensity of the signals and were determined on the basis of the following criteria: −, not detected at more than the background level; +/−, expression was observed but close to detection limit; +, ++, and +++; distinct expression with different intensities. We often observed ISH signals in sparsely scattered cells (denoted as S). For 5-HT1B and 5-HT2A receptor mRNAs, to represent their very high specificity for layer IVCbeta, ++++ was used. For 5-HT1A receptor mRNA, its expression in layers II and III of V1 was observed only at the border between layers I and II (denoted as B). For 5-HT1F receptor mRNA, weak but consistent signals were observed at the border between layers IVCbeta and VA and we are not certain as to which layer this signal belongs to (denoted as #). For 5-HT7 receptor mRNA, very weak signals were observed in the LGN in a few scattered cells that appeared to be interneurons (denoted as I).

effect of CP93129, whereas the remaining 12 neurons, no effect. To confirm that the effect of CP93129 is receptor-mediated, we coadministered the 5-HT1B receptor-specific antagonist SB216641. SB216641 antagonized the effects of CP93129 in all the 5 neurons tested, including both facilitated and suppressed neurons (data not shown).

Although CP93129 showed both facilitative and suppressive effects, we noted that all the neurons, except for 1 that were suppressed by the 5-HT1B agonist had small response magnitude. The part of the graph corresponding to the response magnitude less than 50 spikes/s (shown with a dotted line in Fig. 7A) was enlarged in Figure 7B. In this graph, all the neurons suppressed by CP93129 exhibited firing rates lower than 13 spikes/s. To examine whether the incidence of each type of response modulation depends on the difference of firing rate of neurons, we classified neurons showing significant response modulation into 2 groups according to firing rate, either higher or lower than 13 spikes/s, and performed Fisher's exact test. However, the difference was not at statistically significant level ($P = 0.098$) in spite of the high incidence of suppressed neurons in low firing group, which was owing to 1 neuron that showed high firing rates (an average of 82.5 spikes/s) at control but it showed suppressive modulation. Thus, we speculate that CP93129 mainly facilitated the visual responses of V1 neurons but tended to suppress a population of neurons with low firing rates.

This raised a possibility that the sign of the modulatory effects of CP93129 is dependent on the neuron's response level. To test this hypothesis, we changed the response magnitude of the recorded neuron by changing contrast of stimuli presented and examined whether CP93129 has differential effects on single neurons with different activity levels. Figure 7C depicts the PSTHs that show visual responses of a V1 neuron to a drifting sinusoidal-grating patch at 2 stimulus contrasts of 20% (right) and 100% (left) in 3 drug conditions; control, during iontophoresis of CP93129, and

recovery from the drug effect. In this example, CP93129 clearly facilitated the responses at high grating contrast (100%) but suppressed them at low grating contrast (20%). The effects of CP93129 on the stimulus contrast-response relationship was tested for the same neuron (Fig. 7D). This example demonstrates that the activation of 5-HT1B receptors facilitates the responses to high-contrast (≥30%) stimulation, but is suppressive or ineffective for responses to low-contrast stimulation (≤20%). Similar response-dependent effects of CP93129 were observed for all the 3 neurons tested, including the one shown in Figure 7C,D.

The firing-rate–dependent effects of CP93129 may improve the signal-to-noise ratio (S/N ratio) of activity of V1 neurons. To test this point, we calculated the S/N ratio as the ratio of the number of spikes in the visual response to spontaneous discharge which was added by 1 [S/N = (visual response)/(spontaneous discharge + 1)] because our sample included neurons without spontaneous discharge (0 spikes/s). The S/N ratio was calculated for the 24 neurons which were facilitated by CP93129, and was significantly larger during drug administration than control (Wilcoxon signed-rank test, $P < 0.01$). Thus, our results suggest that the effect of the 5-HT1B receptor agonist is dependent on the response level of each neuron, and that it improves S/N ratio of visual input from the LGN to the cortex.

Next, we examined the effects of the 5-HT2A agonist, DOI, on visual responses. Results were very intriguing because DOI also exerted bidirectional modulatory effects on the neuron's firing rate, but the sign of response modulation was opposite that of the 5-HT1B receptor agonist CP93129. Figure 8A,B shows a summary of the modulatory effects of DOI on 44 neurons. Most of the facilitative effects (12/44 cells) were concentrated in neurons that exhibited firing rates lower than 25 spikes/s. On the other hand, suppressive effects (9/44 cells) were more often observed in neurons with firing rates higher than 25 spikes/s. Therefore, to examine the relationship between the incidence of the type of response modulation by
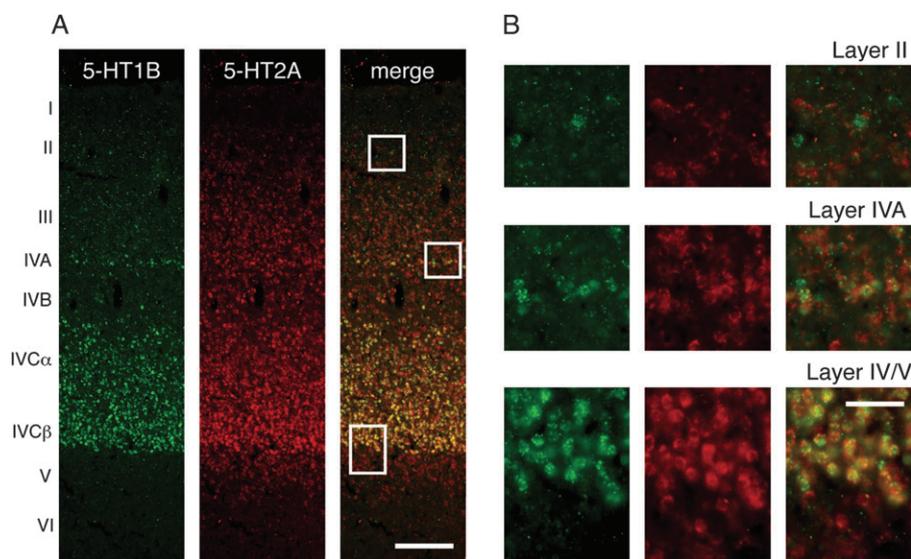
Figure 4. Double ISH of 5-HT1B and 5-HT2A receptor genes in monkey V1. (*A*) Double ISH with 5-HT1B (green) and 5-HT2A (red) gene probes. The white boxes in layers II, IVA, and IV/V are magnified in (*B*). Bar: 200 μm. (*B*) A higher magnification view of the white boxes in (*A*). Note that most of the 5-HT1B–positive neurons coexpress 5-HT2A receptor mRNA in layers IVA and IVC, but not necessarily so in layer II. Bar: 50 μm.
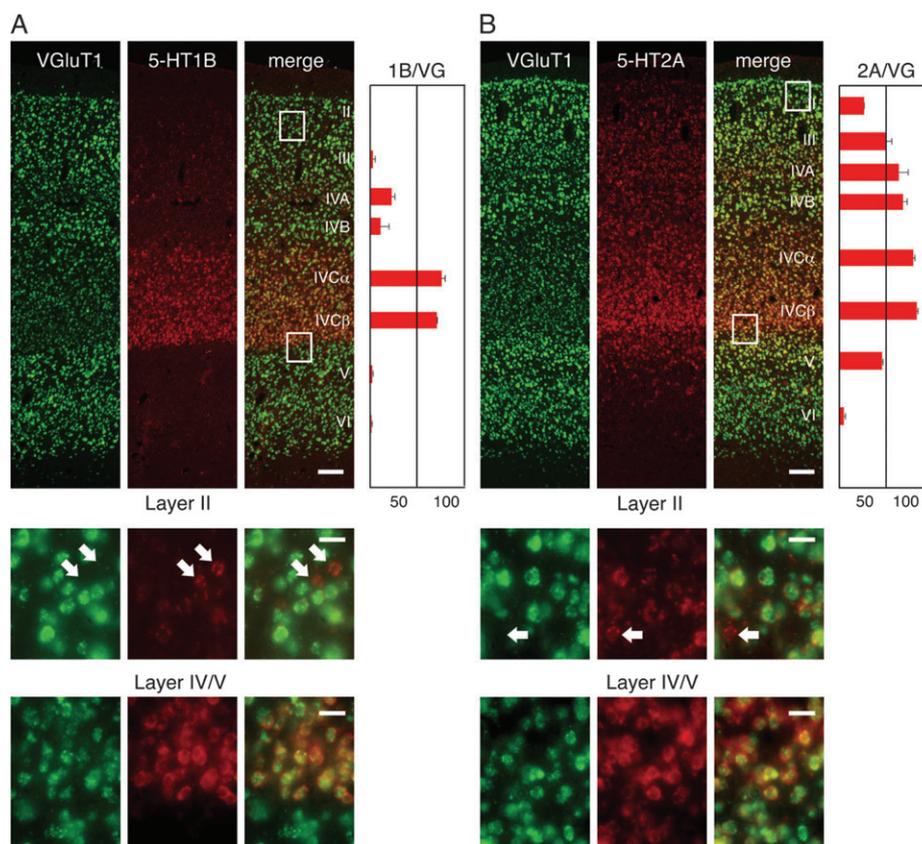

Figure 5. Double ISH of 5-HT1B/2A receptor and VGluT1 gene probes in monkey V1. (*A*) Double ISH with 5-HT1B (red) and VGluT1 (green) gene probes. Bar: 100 μm. The white box in layer II and that at the border between layers IV and V, respectively, are magnified below. White arrows indicate the 5-HT1B receptor mRNA-positive neurons with no detectable expression of VGluT1 mRNA. Bar: 20 μm. The ratios of the neurons that express 5-HT1B receptor mRNA among the VGluT1-positive excitatory neurons (1B/VG) in layers II, III, IVA, IVB, IVCalpha, IVCbeta, V, and VI are shown by a bar graph on the right side of panel A. Error bars are SEM (*n* = 3). (*B*) Double ISH with 5-HT2A (red) and VGluT1 (green) gene probes. The red signals represent 5-HT2A receptor mRNA. The other descriptions are the same as in panel A. Note that the ratio of the 5-HT2A–positive neurons in the bar graph is high in the upper layers as well. In these upper layers, we generally detected a lower level of 5-HT2A receptor mRNA per cell, compared with that in layer IVC.
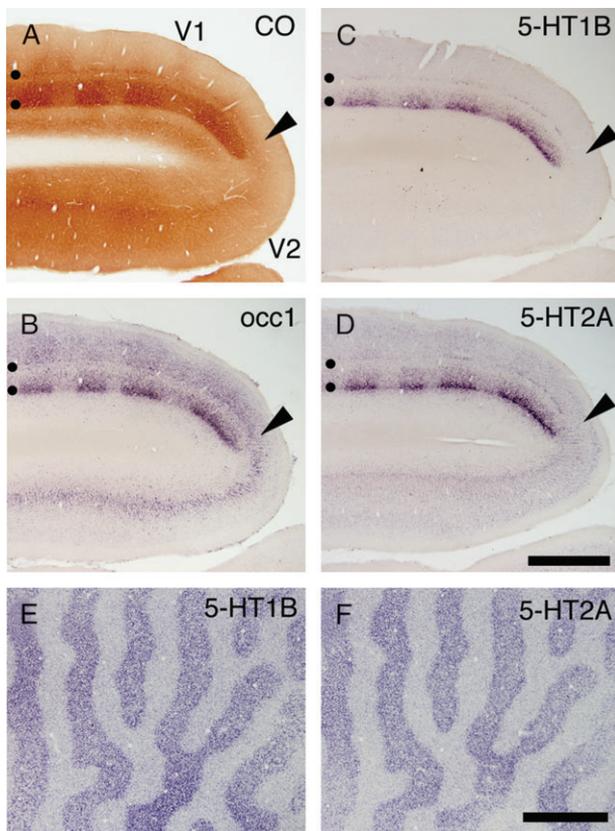
Figure 6. Expressions of 5-HT1B and 5-HT2A receptor mRNAs in V1 following monocular inactivation. TTX was injected into 1 eye twice a week for 21 days (*A–D*), or 3 h before sacrifice (*E,F*). These monocularly inactivated monkey brains were histochemically analyzed. (*A*) CO staining near V1-V2 border (shown by the black arrowheads). (*B–D*) ISH in V1 and V2. (*B*) *occ1*, (*C*) 5-HT1B receptor, (*D*) 5-HT2A receptor. Adjacent sections were analyzed in this order. Black circles in panels (*A–D*) indicate layers IVA and IVCbeta. (*E* and *F*) 5-HT1B and 5-HT2A receptor mRNA expressions were examined by ISH after 3 h monocular inactivation (MD). These photos show tangential sections at the level of layer IVC. Note that 5-HT1B and 5-HT2A receptor mRNAs exhibit almost identical patterns. Scale bars: 500 μm.

DOI and the class of firing rate demarcated at 25 spikes/s, we performed Fisher's exact test and found statistically significant difference among those factors ($P < 0.01$). This analysis showed that DOI facilitates visual responses of neurons with a low firing rate but suppresses those of neurons with a high firing rate.

However, DOI shows an affinity not only for 5-HT2A but also for 5-HT2B/2C (Barnes and Sharp 1999). To confirm that the modulatory effect by DOI is mediated by 5-HT2A receptors, we tested the effect of ketanserin, a highly selective antagonist of the 5-HT2A receptors (Barnes and Sharp 1999), on endogenous serotonin (Fig. 8*C,D*). On the basis of the results of DOI, we expected that ketanserin would block the facilitative effect of the endogenous serotonin on neurons with low firing rates. Indeed, the suppressive effect of ketanserin was mostly observed in neurons with firing rates lower than 25 spikes/s. Ketanserin also showed a facilitative effect on 1 neuron with a high firing rate. Thus, we conclude that 5-HT2A receptors show response-dependent modulatory effects, but that its effects are opposite those of 5-HT1B receptors.

Finally, we show the laminar distributions of the effects of CP93129, DOI and kentanserin (summarized in Table 2). In contrast to the highly layer-specific distribution of 5-HT1B and 5-HT2A receptor mRNAs, we found no difference in drug effect between layer IVC and other layers (Fisher's exact test, CP93129, $P = 0.60$; DOI, $P = 0.47$; ketanserin, $P = 1.00$). Although the numbers of sampled cells are relatively small, the facilitative and suppressive effects of CP93129 and DOI were evenly distributed across layers.

Discussion

In this study, we report that 5-HT1B and 5-HT2A receptor mRNAs are highly enriched in the geniculorecipient layers in macaque V1. Studies by us as well as by other researchers indicate that this expression pattern is not observed in nonprimate mammals, suggesting species-specific (perhaps primate-specific) roles of 5-HT1B and 5-HT2A receptors in visual processing. Our in vivo electrophysiological experiments demonstrated that the 5-HT1B and 5-HT2A agonists exert modulatory effects on the responses of V1 neurons in macaque monkeys. These data suggest a correlation between area-specific gene expression and functional properties.

Distribution of 5-HT1B Receptor mRNA and Proteins in V1

In contrast to the highly specific localization of the 5-HT1B receptor mRNA in the geniculorecipient layers, the effects of receptor agonists were observed throughout all 6 layers in V1 suggesting a wider distribution of the receptor proteins than that of the mRNA. Consistent with this observation, previous radioligand binding studies demonstrate wide-spread distribution of the 5-HT binding sites within the monkey V1 (Rakic et al. 1988; Parkinson et al. 1989). Although we do not have our own experimental data, many reports suggest presynaptic localization of 5-HT1B receptor protein (Mooney et al. 1994; Ghavami et al. 1999; Riad et al. 2000; Laurent et al. 2002; also see Sari 2004 for a review). Especially, Varnäs et al. (2005) found a high level mRNA expression of 5-HT1B receptor gene, but very low level receptor binding sites in the LGN of humans, suggesting that the 5-HT1B receptor protein produced in the LGN may be transported to the presynaptic sites in the visual cortex. Similarly, 5-HT1B receptor proteins produced in layers IVA and IVC may well be distributed widely across layers, because the neurons in these layers participate in interlaminar processing, both supra- and infragranular (Lund 1988). However, it is also possible that the accumulation of mRNA is not proportional to that of the protein because additional regulation at the level of translation and turnover rates may be present.

Compared with the 5-HT1B receptor, 5-HT2A receptor mRNA was detected more widely across layers (Fig. 5*B*), which is consistent with the electrophysiological result (Table 2). Regarding this point, previous reports suggest postsynaptic localization of the 5-HT2A receptors (Rakic et al. 1988; Lópéz-Giménez et al. 2001; Miner et al. 2003). The subcellular localizations of the 5-HT1B and 5-HT2A receptor proteins have an important implication on the differential roles of these receptors in modulating visual processing in the early visual system. Further study is needed to understand the subcellular localization of 5-HT1B receptor proteins and their physiological effects in V1.

Activity-Dependent and V1-Specific Expression of 5-HT Receptor Genes in Primates

Although activity-dependency clearly plays an important role in determining the distribution patterns of the 5-HT1B and
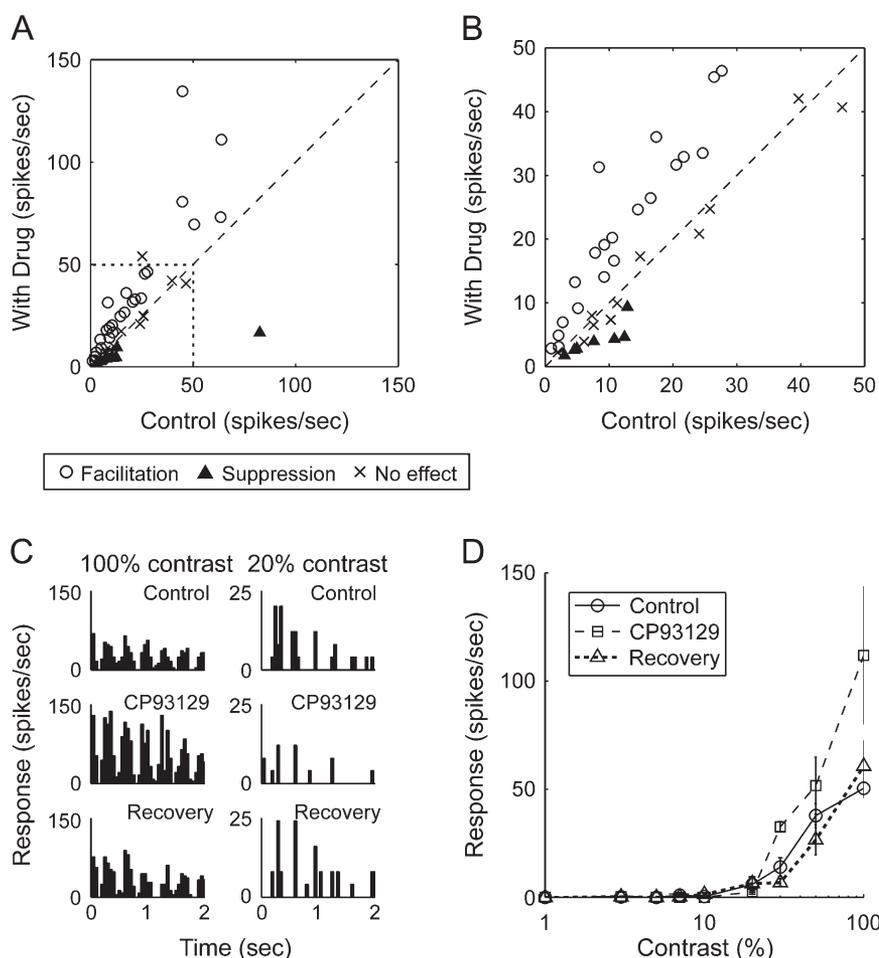
Figure 7. Effects of 5-HT1B agonist, CP93129, on visual responses of neurons in macaque V1. (*A*) Effects of CP93129 on firing rates of 45 V1 neurons. Firing rates under drug-administered condition (ordinate) were plotted against those of control responses (average of responses during the control and recovery conditions) (abscissa). Symbols indicate effects of CP93129 (open circle, facilitation; cross, no effect; filled triangle, suppression). (*B*) Part of the graph shown in *A* (shown by a dotted line in *A*) is indicated with enlarged scales. (*C*) PSTHs of visual responses of a V1 neuron to a drifting sinusoidal-grating patch at 2 stimulus contrasts of 20% (right) and 100% (left) in 3 drug conditions; control, during iontophoresis of CP93129, and recovery from the drug effect. (*D*) Effects of CP93129 on contrast-response function of a complex cell in layer 4B. Circles, squares, and triangles are averaged responses (±SEM) to the visual stimulus at each grating contrast before, during, and after drug administration, respectively.

5-HT2A receptor mRNAs, "activity" alone is not sufficient to account for their high area/lamina specificity. Many genes under activity-dependent regulation have been reported (e.g., GAD67, Gamma-aminobutyric acid (GABA) receptors, CAMKs, NRF, zif268; Jones 1990; Benson et al. 1991; Huntsman et al. 1994; Chaudhuri et al. 1995; Tighilet et al. 1998; Nie and Wong-Riley 1999; Guo et al. 2000). Nevertheless, the expression of these genes is neither lamina nor area specific (e.g., Okuno et al. 1997). The expression patterns of *occ1*, 5-HT1B, and 5-HT2A receptor genes could be explained if their transcriptions are upregulated only by retinal inputs but not by other factors. We found that both the 5-HT1B and 5-HT2A receptor mRNAs exhibit a very rapid response to the loss of retinal activity, comparable to that of immediate-early genes such as c-*fos* and *zif268* (Knapska and Kaczmarek 2004). The high turnover rate of the two 5-HT receptors may be appropriate for adjusting the visual cortical functions to change of environment, for example, diurnal rhythm. In addition, however, there may exist cell-type specific gene regulation to achieve such a specific expression in V1.

The expression patterns of 5-HT1B receptor mRNA reported in this study are quite different from those reported for nonprimate mammals (Boschert et al. 1994; Bruinvels et al. 1994; Bonaventure et al. 1998). We also examined the expressions of 5-HT1B and 5-HT2A receptor mRNAs in marmosets (a New World monkey), ferrets and cats, in addition to rats and mice, and found similar V1 specificity in only marmosets (data not shown). In postmortem human brains, 5-HT1B receptor mRNA is enriched in the middle layers of the occipital cortex (putative visual area) and the upper layers of most other areas, the lamina pattern of which is reminiscent of that in monkeys (Varnäs et al. 2005). Although the reported area difference in humans does not appear to be so conspicuous compared with that in monkeys, this may be due to a long postmortem period before fixation (>29 h) or to age difference, whereas the processing of monkey samples by trans-cardiac perfusion fixation is very rapid. From these observations, we consider that the activity-dependent expressions of 5-HT1B and 5-HT2A receptor mRNAs in adult geniculorecipient layers may be a characteristic feature of the primate cortex. Further comparative studies would prove this.

It is intriguing that a set of molecules, *occ1*, 5-HT1B, and 5-HT2A receptor mRNAs show V1-enriched expression and are under similar activity-dependent regulation. It is quite possible
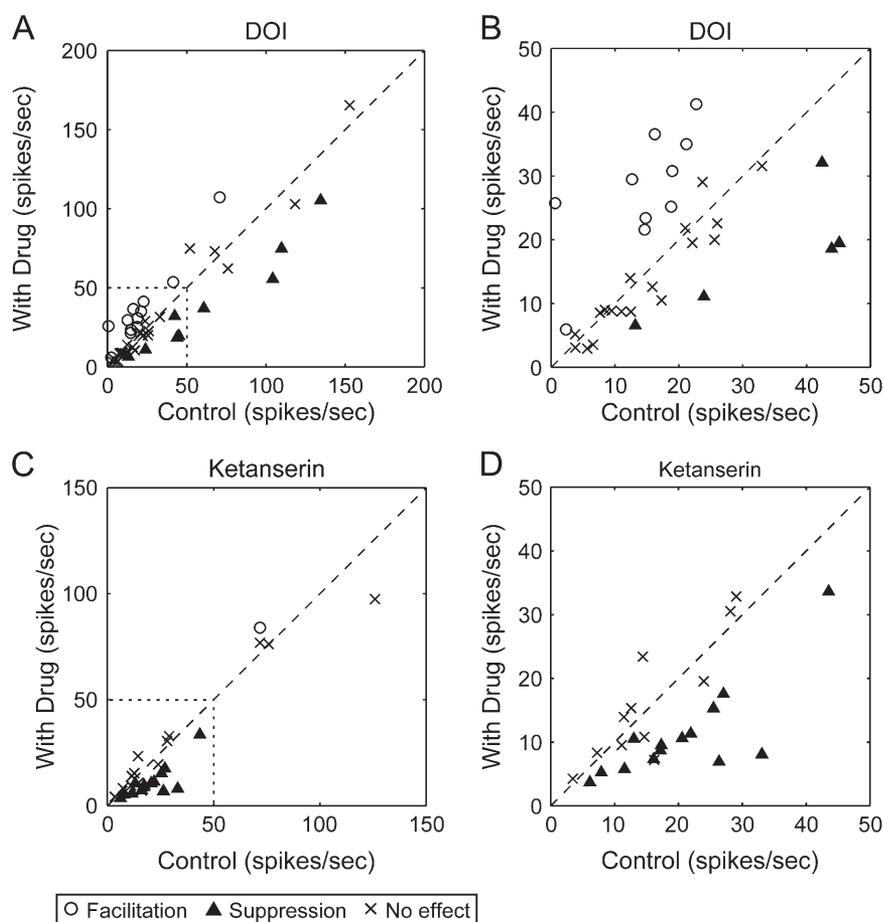
Figure 8. Effects of 5-HT2A agonist DOI and antagonist ketanserin on visual responses of neurons in macaque V1. (*A*) Effects of DOI on firing rates of 44 neurons in V1. Firing rates under drug-administered condition (ordinate) were plotted against those of control responses (average of responses before and after iontophoretic administration) (abscissa). Symbols indicate effects of DOI (open circle, facilitation; cross, no effect; filled triangle, suppression). (*B*) Part of the graph shown in (*A*) (shown by a dotted line in *A*) is indicated with enlarged scales. (*C*) The effects of ketanserin on the firing rate of 44 V1 neurons. Firing rates during drug condition (ordinate) were plotted against that of control responses (the average of responses before and after iontophoretic administration) (abscissa). Symbols indicate effects of ketanserin (open circle, facilitation; cross, no effect; filled triangle, suppression). (*D*) Enlarged part of the graph shown with dotted line in (*C*).

that these molecules work cooperatively in the monkey V1 in response to incoming inputs. Although the specific function of the occ1 molecule is yet unknown, this gene belongs to a family of extracellular matrix proteins, some of which are known to affect ocular dominance plasticity in rodents (Berardi et al. 2003). 5-HT1B and 5-HT2A receptors affect synaptic transmission, as we have shown in this paper. In addition, they may also affect synaptic plasticity by regulating downstream signal transduction pathways. For example, 5-HT1B receptors are considered to be negatively coupled to adenylate cyclase (reviewed in Sari 2004), whereas 5-HT2A receptors recruit phospholipase C, pertussis toxin–sensitive heterotrimeric G(i/o) proteins, and Src signaling (Gonzalez-Maeso et al. 2007). The enriched expressions of these molecules in response to visual inputs could cause or modulate plasticity in the primate V1.

Table 2

Lamina distribution of recorded neurons in the electrophysiological experiments

Layer	2/3	4B	4C	5/6	Unknown	Total
CP93129						
Facilitation	7	7	5	5	1	25 (56%)
Suppression	2	0	2	2	2	8 (17%)
No effect	3	0	6	1	2	12 (27%)
Total	12	7	13	8	5	45
DOI						
Facilitation	2	4	2	1	3	12 (27%)
Suppression	3	2	0	4	0	9 (20%)
No effect	7	3	1	8	4	23 (52%)
Total	12	9	3	13	7	44
Ketanserin						
Facilitation	1	0	0	0	0	1 (3%)
Suppression	3	1	3	5	3	15 (51%)
No effect	2	0	2	8	1	13 (45%)
Total	6	1	5	13	4	29

Firing-Rate–Dependent Effect of 5-HT1B/2A Agonists In Vivo

The electrophysiological study revealed the complexity of the in vivo effects mediated by the 5-HT1B and 5-HT2A receptors. We found that each receptor can exert both suppressive and facilitative effects, depending on the firing rate of the recorded neurons. Regarding the 5-HT1B receptor, an analogous

context-dependent bidirectional modulation has been reported in in vitro preparations of brain slices containing the optic tract and the LGN (Seeburg et al. 2004) or the ventral posteriomedial nucleus of thalamus and the somatosensory cortex (Laurent et al. 2002). For example, Seeburg et al. (2004) reported that 5-HT1B receptor–mediated serotonergic modulation of responses in LGN neurons to stimulation of optic tract is

dependent on the temporal frequency of the stimulus. The net effect of the 5-HT1 receptor agonist on retinogeniculate transmission is suppressive for low-frequency inputs, but rather ineffective or facilitative for high-frequency inputs. They suggested that the alleviation of synaptic depression caused by high-frequency stimulation may underlie such effects of the 5-HT1B receptors.

The effects of the 5-HT2A receptors, on the other hand, should be explained by a different mechanism, because 5-HT2A receptor activation is considered to cause phospholipase C–mediated synaptic facilitation by reducing outward potassium current (Barnes and Sharp 1999; Lambe and Aghajanian 2001). An activation of 5-HT2A receptor has been known to exert direct facilitative actions on not only pyramidal neurons but also interneurons (Araneda and Andrade 1991; Tanaka and North 1993), by which neighboring pyramidal neurons are indirectly inhibited (Sheldon and Aghajanian 1991; Marek and Aghajanian 1996; Zhou and Hablitz 1999). Therefore, serotonin probably has complex influences by controlling the relative activity of excitatory and inhibitory neurons within local circuitry via 5-HT1B and 5-HT2A receptors.

Physiological Significance of Serotonergic Modulation in Visual System

Serotonergic fibers that arise from the dorsal and median raphe nuclei (Schofield and Everitt 1981; Sladek et al. 1982) innervate the neocortex including the visual cortex of the primate (Morrison et al. 1982; Doty 1983; Foote and Morrison 1984; de Lima et al. 1988; Wilson and Molliver 1991) and the cat (Jonsson and Kasamatsu 1983). Raphe nuclei in cats or rats have been shown to change their activity pattern according to the level of behavioral arousal across the sleep–wake–arousal cycle (McGinty and Harper 1976; Lydic et al. 1983; Guzman-Marin et al. 2000). In addition, the 5-HT release in V1 could be regulated locally by 5-HT1B autoreceptors on the presynaptic terminals of the raphe nucleus that innervate V1 (for a review, Sari 2004) or potentially by the activity from the prefrontal cortex (Celada et al. 2001). The effect of serotonin in the cortex should, thus, depend on the dynamic regulation of the level of serotonin and the receptors.

Although the enhanced expression of 5-HT1B receptor mRNA in the LGN and V1 suggests its primary role in the visual system, it was also expressed widely in the thalamus (Fig. 2, supporting Fig. S1). Weak but significant cortical expression was concentrated in the thalamocortical input layers of the primary sensory (auditory and somatosensory) areas (Figs 2 and 3, supporting Fig. S1). The roles of serotonin in V1 might thus be regarded as an enhancement of a general role of serotonin in the modulation of thalamocortical transmission.

In this study, we demonstrate that the activation of 5-HT1B receptors in V1 generally facilitates visual responses but tends to suppress weak responses. This suggests that, in geniculocortical transmission, nonsynchronized spontaneous activity (noise) from the LGN neurons would be reduced by the suppressive effect of 5-HT1B receptors, but the visually evoked synchronized signals would be preserved or efficiently transferred to V1, thus, enhancing the S/N ratio in input–output relationship. On the other hand, neurons in the input layers of V1, which abundantly express the 5-HT2A receptor may act as a gain controller by enhancing weak signal response and suppressing excessive response. We therefore suggest that, serotonin release in V1

exerts coordinated modulatory effects through 5-HT1B and 5-HT2A receptors on the V1 neurons. It is therefore possible that the serotonin system has contributed to the evolution of the elaborated function of the primate visual system.

Supplementary Material

Funding

Notes

References

Akasaki T, Sato H, Yoshimura Y, Ozeki H, Shimegi S. 2002. Suppressive effects of receptive field surround of neuronal activity in the cat primary visual cortex. Neurosci Res. 43:207–220.

Araneda R, Andrade R. 1991. 5-Hydroxytryptamine2 and 5-hydroxytryptamine 1A receptors mediate opposing responses on membrane excitability in rat association cortex. Neuroscience. 40:399–412.

Barnes NM, Sharp T. 1999. A review of central 5-HT receptors and their function. Neuropharmacology. 38:1083–1152.

Baumgarten HG, Gothert M. 1997. Serotoninergic neurons and 5-HT receptors in the CNS. Berlin: Springer.

Bellocchio EE, Reimer RJ, Fremeau RTJ, Edwards RH. 2000. Uptake of glutamate into synaptic vesicles by an inorganic phosphate transporter. Science. 289:957–960.

Benson DL, Isackson PJ, Gall CM, Jones EG. 1991. Differential effects of monocular deprivation on glutamic acid decarboxylase and type II calcium-calmodulin-dependent protein kinase gene expression in the adult monkey visual cortex. J Neurosci. 11:31–47.

Berardi N, Pizzorusso T, Ratto GM, Maffei L. 2003. Molecular basis of plasticity in the visual cortex. Trends Neurosci. 26:369–378.

Bonaventure P, Voorn P, Luyten WH, Jurzak M, Schotte A, Leysen JE. 1998. Detailed mapping of serotonin 5-HT1B and 5-HT1D receptor messenger RNA and ligand binding sites in guinea-pig brain and trigeminal ganglion: clues for function. Neuroscience. 82:469–484.

Boschert U, Amara DA, Segu L, Hen R. 1994. The mouse 5-hydroxytryptamine1B receptor is localized predominantly on axon terminals. Neuroscience. 58:167–182.

Bruinvels AT, Landwehrmeyer B, Gustafson EL, Durkin MM, Mengod G, Branchek TA, Hoyer D, Palacios JM. 1994. Localization of 5-HT1B, 5-HT1D alpha, 5-HT1E and 5-HT1F receptor messenger RNA in rodent and primate brain. Neuropharmacology. 33:367–386.

Burnet PW, Eastwood SL, Lacey K, Harrison PJ. 1995. The distribution of 5-HT1A and 5-HT2A receptor mRNA in human brain. Brain Res. 676:157–168.

Callaway EM. 1998. Local circuits in primary visual cortex of the macaque monkey. Annu Rev Neurosci. 21:47–74.

Celada P, Puig MV, Casanovas JM, Guillazo G, Artigas F. 2001. Control of dorsal raphe serotonergic neurons by the medial prefrontal cortex: involvement of serotonin-1A, GABA(A), and glutamate receptors. J Neurosci. 21:9917–9929.

Chaudhuri A, Matsubara JA, Cynader MS. 1995. Neuronal activity in primate visual cortex assessed by immunostaining for the transcription factor Zif268. Vis Neurosci. 12:35–50.

de Lima AD, Bloom FE, Morrison JH. 1988. Synaptic organization of serotonin-immunoreactive fibers in primary visual cortex of the macaque monkey. J Comp Neurol. 274:280–294.

Doty RW. 1983. Nongeniculate afferents to striate cortex in macaques. J Comp Neurol. 218:159–173.

Felleman DJ, Van Essen DC. 1991. Distributed hierarchical processing in the primate cerebral cortex. Cereb Cortex. 1:1–47.

Foote SL, Morrison JH. 1984. Postnatal development of laminar innervation patterns by monoaminergic fibers in monkey (Macaca fascicularis) primary visual cortex. J Neurosci. 4:2667–2680.

Ghavami A, Stark KL, Jareb M, Ramboz S, Segu L, Hen R. 1999. Differential addressing of 5-HT1A and 5-HT1B receptors in epithelial cells and neurons. J Cell Sci. 112:967–976.

Gonzalez-Maeso J, Weisstaub NV, Zhou M, Chan P, Ivic L, Ang R, Lira A, Bradley-Moore M, Ge Y, Zhou Q, et al. 2007. Hallucinogens recruit specific cortical 5-HT(2A) receptor-mediated signaling pathways to affect behavior. Neuron. 53:439–452.

Guo A, Nie F, Wong-Riley M. 2000. Human nuclear respiratory factor 2 alpha subunit cDNA: isolation, subcloning, sequencing, and in situ hybridization of transcripts in normal and monocularly deprived macaque visual system. J Comp Neurol. 417:221–232.

Guzman-Marin R, Alam MN, Szymusiak R, Drucker-Colin R, Gong H, McGinty D. 2000. Discharge modulation of rat dorsal raphe neurons during sleep and waking: effects of preoptic/basal forebrain warming. Brain Res. 875:23–34.

Hendrickson AE, Tillakaratne NJ, Mehra RD, Esclapez M, Erickson A, Vician L, Tobin AJ. 1994. Differential localization of two glutamic acid decarboxylases (GAD65 and GAD67) in adult monkey visual cortex. J Comp Neurol. 343:566–581.

Hoyer D, Hannon JP, Martin GR. 2002. Molecular, pharmacological and functional diversity of 5-HT receptors. Pharmacol Biochem Behav. 71:533–554.

Hubel DH, Wiesel TN. 1977. Ferrier lecture. Functional architecture of macaque monkey visual cortex. Proc R Soc Lond B Biol Sci. 198:1–59.

Huntsman MM, Isackson PJ, Jones EG. 1994. Lamina-specific expression and activity-dependent regulation of seven GABAA receptor subunit mRNAs in monkey visual cortex. J Neurosci. 14:2236–2259.

Jin H, Oksenberg D, Ashkenazi A, Peroutka SJ, Duncan AM, Rozmahel R, Yang Y, Mengod G, Palacios JM, O'Dowd BF. 1992. Characterization of the human 5-hydroxytryptamine1B receptor. J Biol Chem. 267:5735–5738.

Jones EG. 1990. The role of afferent activity in the maintenance of primate neocortical function. J Exp Biol. 153:155–176.

Jonsson G, Kasamatsu T. 1983. Maturation of monoamine neurotransmitters and receptors in cat occipital cortex during postnatal critical period. Exp Brain Res. 50:449–458.

Knapska E, Kaczmarek L. 2004. A gene for neuronal plasticity in the mammalian brain: Zif268/Egr-1/NGFI-A/Krox-24/TIS8/ZENK? Prog Neurobiol. 74:183–211.

Komatsu Y, Watakabe A, Hashikawa T, Tochitani S, Yamamori T. 2005. Retinol-binding protein gene is highly expressed in higher-order association areas of the primate neocortex. Cereb Cortex. 15:96–108.

Lambe EK, Aghajanian GK. 2001. The role of Kv1.2-containing potassium channels in serotonin-induced glutamate release from thalamocortical terminals in rat frontal cortex. J Neurosci. 21:9955–9963.

Laurent A, Goaillard JM, Cases O, Lebrand C, Gaspar P, Ropert N. 2002. Activity-dependent presynaptic effect of serotonin 1B receptors on

the somatosensory thalamocortical transmission in neonatal mice. J Neurosci. 22:886–900.

Lopéz-Giménez JF, Vilaro MT, Palacios JM, Mengod G. 2001. Mapping of 5-HT2A receptors and their mRNA in monkey brain: [3H]MDL100,907 autoradiography and in situ hybridization studies. J Comp Neurol. 429:571–589.

Lund JS. 1988. Anatomical organization of macaque monkey striate visual cortex. Annu Rev Neurosci. 11:253–288.

Lydic R, McCarley RW, Hobson JA. 1983. Enhancement of dorsal raphe discharge by medial pontine reticular formation stimulation depends on behavioral state. Neurosci Lett. 38:35–40.

Marek GJ, Aghajanian GK. 1996. LSD and the phenethylamine hallucinogen DOI are potent partial agonists at 5-HT2A receptors on interneurons in rat piriform cortex. J Pharmacol Exp Ther. 278:1373–1382.

McGinty DJ, Harper RM. 1976. Dorsal raphe neurons: depression of firing during sleep in cats. Brain Res. 101:569–575.

Miner LA, Backstrom JR, Sanders-Bush E, Sesack SR. 2003. Ultrastructural localization of serotonin2A receptors in the middle layers of the rat prelimbic prefrontal cortex. Neuroscience. 116: 107–117.

Mooney RD, Shi MY, Rhoades RW. 1994. Modulation of retinotectal transmission by presynaptic 5-HT1B receptors in the superior colliculus of the adult hamster. J Neurophysiol. 72:3–13.

Morrison JH, Foote SL, Molliver ME, Bloom FE, Lidov HG. 1982. Noradrenergic and serotonergic fibers innervate complementary layers in monkey primary visual cortex: an immunohistochemical study. Proc Natl Acad Sci USA. 79:2401–2405.

Nie F, Wong-Riley M. 1999. Nuclear respiratory factor-2 subunit protein: correlation with cytochrome oxidase and regulation by functional activity in the monkey primary visual cortex. J Comp Neurol. 404:310–320.

Northcutt RG, Kaas JH. 1995. The emergence and evolution of mammalian neocortex. Trends Neurosci. 18:373–379.

Okuno H, Kanou S, Tokuyama W, Li YX, Miyashita Y. 1997. Layerspecific differential regulation of transcription factors Zif268 and Jun-D in visual cortex V1 and V2 of macaque monkeys. Neuroscience. 81:653–666.

Ozeki H, Sadakane O, Akasaki T, Naito T, Shimegi S, Sato H. 2004. Relationship between excitation and inhibition underlying size tuning and contextual response modulation in the cat primary visual cortex. J Neurosci. 24:1428–1438.

Parkinson D, Coscia EC, Daw NW. 1989. Identification and localization of 5-hydroxytryptamine receptor sites in macaque visual cortex. Vis Neurosci. 2:515–525.

Pickard GE, Smith BN, Belenky M, Rea MA, Dudek FE, Sollars PJ. 1999. 5-HT1B receptor-mediated presynaptic inhibition of retinal input to the suprachiasmatic nucleus. J Neurosci. 19:4034–4045.

Rakic P, Goldman-Rakic PS, Gallager D. 1988. Quantitative autoradiography of major neurotransmitter receptors in the monkey striate and extrastriate cortex. J Neurosci. 8:3670–3690.

Riad M, Garcia S, Watkins KC, Jodoin N, Doucet E, Langlois X, el Mestikawy S, Hamon M, Descarries L. 2000. Somatodendritic localization of 5-HT1A and preterminal axonal localization of 5-HT1B serotonin receptors in adult rat brain. J Comp Neurol. 417:181–194.

Sari Y. 2004. Serotonin 1B receptors: from protein to physiological function and behavior. Neurosci Biobehav Rev. 28:565–582.

Sato H, Katsuyama N, Tamura H, Hata Y, Tsumoto T. 1996. Mechanisms underlying orientation selectivity of neurons in the primary visual cortex of the macaque. J Physiol. 494:757–771.

Schofield SP, Everitt BJ. 1981. The organization of indoleamine neurons in the brain of the rhesus monkey (Macaca mulatta). J Comp Neurol. 197:369–383.

Seeburg DP, Liu X, Chen C. 2004. Frequency-dependent modulation of retinogeniculate transmission by serotonin. J Neurosci. 24: 10950–10962.

Sheldon PW, Aghajanian GK. 1991. Excitatory responses to serotonin (5-HT) in neurons of the rat piriform cortex: evidence for mediation by 5-HT1C receptors in pyramidal cells and 5-HT2 receptors in interneurons. Synapse. 9:208–218.

Shintani T, Kato A, Yuasa-Kawada J, Sakuta H, Takahashi M, Suzuki R, Ohkawara T, Takahashi H, Noda M. 2004. Large-scale identification and characterization of genes with asymmetric expression patterns in the developing chick retina. J Neurobiol. 59:34-47.

Sincich LC, Horton JC. 2005. The circuitry of V1 and V2: integration of color, form, and motion. Annu Rev Neurosci. 28:303-326.

Skottun BC, De Valois RL, Grosof DH, Movshon JA, Albrecht DG, Bonds AB. 1991. Classifying simple and complex cells on the basis of response modulation. Vision Res. 31:1079-1086.

Sladek JRJ, Garver DL, Cummings JP. 1982. Monoamine distribution in primate brain-IV. Indoleamine-containing perikarya in the brain stem of Macaca arctoides. Neuroscience. 7:477-493.

Suzuki H, Yaoi T, Kawai J, Hara A, Kuwajima G, Wantanabe S. 1996. Restriction landmark cDNA scanning (RLCS): a novel cDNA display system using two-dimensional gel electrophoresis. Nucleic Acids Res. 24:289-294.

Takahata T, Komatsu Y, Watakabe A, Hashikawa T, Tochitani S, Yamamori T. 2006. Activity-dependent expression of occ1 in excitatory neurons is a characteristic feature of the primate visual cortex. Cereb Cortex. 16:929-940.

Takamori S, Rhee JS, Rosenmund C, Jahn R. 2000. Identification of a vesicular glutamate transporter that defines a glutamatergic phenotype in neurons. Nature. 407:189-194.

Tanaka E, North RA. 1993. Actions of 5-hydroxytryptamine on neurons of the rat cingulate cortex. J Neurophysiol. 69:1749-1757.

Tighilet B, Hashikawa T, Jones EG. 1998. Cell- and lamina-specific expression and activity-dependent regulation of type II calcium/calmodulin-dependent protein kinase isoforms in monkey visual cortex. J Neurosci. 18:2129-2146.

Tochitani S, Liang F, Watakabe A, Hashikawa T, Yamamori T. 2001. The occ1 gene is preferentially expressed in the primary visual cortex in an activity-dependent manner: a pattern of gene expression related to the cytoarchitectonic area in adult macaque neocortex. Eur J Neurosci. 13:297-307.

Van Hooser SD. 2007. Similarity and diversity in visual cortex: is there a unifying theory of cortical computation? Neuroscientist. 13:639-656.

Varnäs K, Hurd YL, Hall H. 2005. Regional expression of 5-HT1B receptor mRNA in the human brain. Synapse. 56:21-28.

Watakabe A, Fujita H, Hayashi M, Yamamori T. 2001. Growth/differentiation factor 7 is preferentially expressed in the primary motor area of the monkey neocortex. J Neurochem. 76:1455-1464.

Watakabe A, Ichinohe N, Ohsawa S, Hashikawa T, Komatsu Y, Rockland KS, Yamamori T. 2007. Comparative analysis of layer-specific genes in Mammalian neocortex. Cereb Cortex. 17:1918-1933.

Wilson MA, Molliver ME. 1991. The organization of serotonergic projections to cerebral cortex in primates: retrograde transport studies. Neuroscience. 44:555-570.

Wong-Riley MT. 1994. Primate visual cortex: dynamic metabolic organization and plasticity revealed by cytochrome oxidase. In: Peters A, Rockland KS, editors. Cerebral cortex. New York: Plenum Press. p. 141-200.

Yamamori T, Rockland KS. 2006. Neocortical areas, layers, connections, and gene expression. Neurosci Res. 55:11-27.

Zarrinpar A, Callaway EM. 2006. Local connections to specific types of layer 6 neurons in the rat visual cortex. J Neurophysiol. 95:1751-1761.

Zhou FM, Hablitz JJ. 1999. Activation of serotonin receptors modulates synaptic transmission in rat cerebral cortex. J Neurophysiol. 82:2989-2999.